



1 **Assessment of vertical air motion among reanalyses and qualitative comparison with direct**  
2 **VHF radar measurements over the two tropical stations**

3 *Kizhathur Narasimhan Uma<sup>1</sup>, Siddarth Shankar Das<sup>1</sup>, Madineni Venkat Ratnam<sup>2</sup>, and Kuniyil*  
4 *Viswanathan Suneeth<sup>1</sup>*

5  
6 <sup>1</sup>Space Physics Laboratory, Vikram Sarabhai Space Centre, ISRO, Trivandrum-695022, India  
7 <sup>2</sup>National Atmospheric Research Laboratory, Dept. of Space, Gadanki-517112, India

8  
9 \*e-mail : urmi\_nmrf@yahoo.co.in

10 **Abstract**

11 Vertical wind ( $w$ ) is one of the most important meteorological parameters for  
12 understanding different atmospheric phenomena. <sup>a range of?</sup> Only Very few direct measurements of  $w$  are  
13 available, <sup>so that?</sup> and most of the time one must depend on reanalysis products. In the present study,  
14 assessment of  $w$  among selected reanalyses, (ERA-Interim, ERA-5, MERRA-2, NCEP-2 and  
15 JRA-55) and qualitative comparison of those datasets with direct VHF radar measurements over  
16 the convectively active regions Gadanki (13.5°N and 79.2°E) and Kototabang (0°S and 100.2°E)  
17 are presented for the first time. The magnitude of  $w$  derived from reanalyses is 10-50% less than  
18 that from the direct radar observations. Radar measurements of  $w$  show downdrafts below 8 to 10  
19 km and updrafts above 8-10 km over both locations. Inter-comparison between the reanalyses  
20 shows that ERAi is <sup>biased high relative to?</sup> overestimating NCEP-2 and <sup>low relative to other?</sup> underestimating all the reanalyses. Directional  
21 tendency shows that the percentage of updrafts captured is reasonably good, but downdrafts are  
22 <sup>poorly?</sup> not well captured by all reanalyses. Thus, caution is advised when using vertical velocities from  
23 reanalyses.

24 **Key Words:** Vertical velocity, MST Radar, Equatorial Atmosphere Radar, Reanalysis

25



## 26 1 Introduction

27 Vertical air motion ( $w$ ) in any region of the Earth's atmosphere reflects the structure and  
28 dynamical features of that region. Importantly, in the lower part of the atmosphere, sudden  
29 widespread changes in weather are usually associated with variations in ~~the~~ vertical air motion.  
30 The magnitude of  $w$  is a factor of ten or more smaller than the horizontal wind; nevertheless, it is  
31 ~~the crucial component for~~ <sup>in</sup> the evolution of severe weather (*Peterson and Balsley, 1979*).  
32 Adiabatic cooling associated with upward motion leads to the formation of clouds and  
33 precipitation and adiabatic warming associated with downward motion leads to the dissipation of  
34 clouds. Extensive studies have been done on the relationships between  $w$  and  
35 precipitation/convection over the tropics (*Back and Bretherton, 2009; Uma and Rao, 2009a; Rao*  
36 *et al., 2009; Uma et al., 2011* and references therein). Thus,  $w$  plays a vital role in controlling  
37 day-to-day changes in weather. Different scales of variability exist in  $w$  <sup>ranging from?</sup> like microscale to meso,  
38 synoptic, and planetary-scales <sup>(space)</sup> (*Uma and Rao, 2009b*). It also controls <sup>conveys? modulates?</sup> the energy and ~~the~~ mass  
39 transport between the upper troposphere and lower stratosphere (*Yamamoto et al., 2007, Rao et*  
40 *al., 2008*). In a nutshell, knowledge of  $w$  <sup>helpful?</sup> is crucial for evaluating virtually all physical processes  
41 in the atmosphere. Hence precise measurements of  $w$  could serve a guiding factor for studying  
42 many processes in the atmosphere.

43 The small magnitudes of  $w$  make it very difficult to measure, as the errors involved in  
44 measurements <sup>often exceed?</sup> are often larger than the actual values. Direct and indirect methods exist to  
45 measure  $w$  (e.g. Doppler measurements using radars for profiling and sonic anemometers in the  
46 boundary layer) as well as indirect computational methods (e.g., adiabatic, kinematic and quasi-  
47 geostrophic vorticity/omega methods). Direct measurements of  $w$  are thus restricted to locations  
48 where radars are situated. Global estimates are derived diagnostically from horizontal winds and  
49 temperatures. Indirect estimation, gives a general view on the distribution of ascending and

①

②

③



50 descending motion on the synoptic scale within the quasi-geostrophic framework (*Tanaka and*  
51 *Yatagai, 2000; Rao et al., 2003*).

52 Reanalyses evaluate the vertical pressure velocity ( $\omega$ ) using indirect estimation (e.g.,  
53 *Dee et al., 2011*). However, reanalyses combine both observations and model outputs to produce  
54 systematic variation in the atmospheric state (e.g., *Fujiwara et al., 2017*). For example, in the  
55 kinematic method,  $\omega$  is estimated by integrating the mass continuity equation assuming  
56 inviscid adiabatic flow. However, this kinematic estimate suffers from errors in the observations  
57 as  $\omega$  is estimated from horizontal divergence (*Tanaka and Yatagai, 2000*). A 10% error in

58 the wind may lead to a 100% error in the estimated divergence (*Holton., 2004*).  $\omega$  from the  
59 thermodynamic energy equation is less sensitive to horizontal winds as it mainly depends on the  
60 temperature gradient. However, in this method the local rate of change in temperature must be  
61 measured accurately, meaning that observations must be taken at frequent intervals in time to  
62 estimate  $\partial T / \partial t$  accurately (*Holton., 2004*). This methodology fails in areas of strong diabatic  
63 heating, especially where condensation and evaporation are involved. The quasi-geostrophic  
64 method for estimating  $\omega$  neglects ageostrophic effects, friction and diabatic heating  
65 (*Stepanyuk et al., 2017*). It is to be noted from the above discussions that reanalyses are not

66 error-free owing to the many underlying approximations and assimilations involved (*Kennedy et*  
67 *al., 2012*).

68 ~~There are few~~ <sup>Other</sup> indirect methods <sup>can be used to</sup> by which we can derive  $w$  from radar measurements in  
69 the middle and upper atmosphere, where direct measurements of vertical wind are not possible  
70 due to technical constraints. These methods include Doppler weather radar, Medium Frequency  
71 (MF) radar and meteor radar. Doppler weather radar uses an indirect method to calculate vertical  
72 winds (*Liou and Chang, 2009; Matejka, 2002*). Meteor radar also cannot determine vertical



73 velocity directly as the winds are determined from meteor showers using a wide beam width. As  
74 a consequence, *Laskar et al.* (2017) calculated vertical wind from meteor wind radar data based  
75 on a “kinematic” method using the continuity equation and hydrostatic balance. *Dowdy et al.*  
76 (2001) have calculated vertical wind using the horizontal momentum and mass continuity  
77 equations from the MF radar data. However, indirect methods are only adopted when direct  
78 methods cannot be used.

79 Very-high frequency (VHF) and ultra-high frequency (UHF) vertical pointing radars are  
80 the most powerful tools for determining ~~the~~ vertical air motion (velocity) directly with high  
81 temporal and vertical resolution. However, the magnitude may still not be directly comparable  
82 between reanalysis products and observations as the reanalyses provide the intensity of vertical  
83 air motion over wide areas ( $> 25 \text{ km}^2$ ), whereas the direct radar measurements provide  
84 information for the column over a single location. Thus, the best way to assess reanalysis  
85 estimates of  $w$  is to compare <sup>a narrower?</sup> ~~its~~ <sup>against radar measurements</sup> directional tendencies ~~with those of radar~~. To the author's  
86 knowledge, no studies yet exist concerning ~~with~~ the assessment of  $w$  products derived from <sup>(8)</sup>  
87 different reanalyses and evaluation of these products against radar measurements. The present  
88 study, <sup>the</sup> which is therefore first of its kind, <sup>(9)</sup> focuses on assessment of  $w$  among various reanalyses  
89 using VHF radar measurements from two tropical stations where convective activity is frequent:  
90 Gadanki (13.5°N and 79.2°E) and Kototabang (0.2°S and 100.2°E). Evaluations of this type are  
91 critically important as reanalysis estimates of  $w$  are widely used by the scientific community to  
92 understand and simulate a variety of atmospheric processes. In section 2, the data and  
93 methodology are described. Section 3 contains the main results followed by a discussion and  
94 summary of the results in section 4.



## 95 2 Data and Methodology

### 96 2.1 Radar measurements

97 Direct measurements of  $w$  are obtained from the Indian Mesosphere-Stratosphere-  
98 Troposphere Radar (IMSTR) located at Gadanki and the Equatorial Atmosphere Radar (EAR)  
99 located at Kototabang. Both the IMSTR and EAR are pulsed coherent radars operating at 53  
100 MHz (IMSTR) and 47 MHz (EAR) respectively. These instruments are used to estimate  $w$  by  
101 measuring the Doppler shift in the vertical beam. The technical details and operational  
102 parameters of the IMSTR have been given by *Rao et al.*, (1995) while those for the EAR have  
103 been given by *Fukao et al.*, (2003).

104 In the present study direct measurements of  $w$  from VHF radars are used to assess  
105 vertical motion between the surface and the lower stratosphere. Data collected from the IMSTR  
106 between 17:30 and 18:30 LT (LT=GMT+5:30 hr) from 1995 to 2015 are analyzed using the  
107 adaptive method (*Anandan et al.*, 2001). This is the common operational mode of the IMSTR for  
108 deriving the winds, and represents the only data available for such a long period of time. In  
109 general, 4-8 vertical profiles are averaged to create <sup>daily mean</sup> daily profiles. Averaging is conducted using  
110 the arithmetic mean as it represents the central tendency, which is generally used for wind  
111 averaging. In a vertically pointing beam, signal-to-noise ratio (SNR) decreases with height  
112 except in ~~areas of~~ stable layer<sup>s</sup> (like the tropopause) and in the presence of strong turbulence.  
113 Above 25 km, the SNR becomes constant in the absence of atmospheric signals. Data in this  
114 region can be therefore treated as noise and used to estimate the threshold SNR (*Uma and Rao*,  
115 2009b). ~~It is found that~~ <sup>estimated in this way</sup> noise levels lie between -17 dB and -19 dB with a  $2\sigma$  value of 3 dB  
116 (where  $\sigma$  is the standard deviation). Thus data having SNR less than -15 dB are discarded from  
117 the present analysis. Data from intense convective days (checked for individual profiles), defined  
118 as  $w$  being less/greater than  $\pm 1 \text{ ms}^{-1}$  are also discarded as these data severely bias the



119 climatological mean vertical velocity (e.g. Uma and Rao, 2009b). The EAR provides quality  
120 check data online (<http://www.rish.kyoto-u.ac.jp/ear/data/index.html>). The EAR operates  
121 continuously and this study uses every <sup>hourly?</sup> hour data (diurnal data of single day) from 2001 to 2015.  
122 The EAR data during convective periods are eliminated following the same criteria as for the  
123 IMSTR, <sup>in</sup> a second screening step. Each full diurnal cycle (after removing convective profiles) is  
124 averaged and considered as a single daily profile for the EAR. For both radars, vertical velocity  
125 (in  $\text{cm s}^{-1}$ ) is directly estimated using equation (1)

$$126 \quad w = -\frac{\lambda}{2} f_d, \quad (1)$$

127 where  $\lambda$  is the radar wavelength (in cm) and  $f_d$  is the Doppler velocity (Hz).

128 It is known that estimates of  $w$  derived from VHF radar measurements are vulnerable to  
129 biases due to tilting layers, strong horizontal winds (e.g., jet-stream), complex topography,  
130 Kelvin-Helmholtz instabilities and gravity waves (Rao et al., 2008 and references therein). Rao  
131 et al., (2008) has discussed in detail the biases that can cause spurious diagnosis of downward  
132 wind as proposed by Nastrom & VanZandt (1994). In addition, they have also discussed the  
133 potential biases caused by beam pointing errors as mentioned by Hauman and Balsley (1996) and  
134 have conducted critical analysis to rule out beam pointing biases from VHF radar data. As  
135 proposed by Nastrom & VanZandt (1994) on the bias caused by gravity waves, Rao et al., (2008)  
136 have investigated biases caused by gravity waves by calculating the variances and found that  
137 downward wind <sup>measurements</sup> below 10 km are essentially unaffected by gravity waves. Their analysis clearly showed  
138 that the mean downward motion below 10 km and upward motion above 10 km are real and not  
139 caused by measurement biases, and also that the <sup>known?</sup> existing biases do not change the direction of  
140 the background  $w$  when measurements are averaged over longer periods.

(1)



A  
introduce how vertical  
velocities are computed  
(i.e. continuity, on  $n$  levels)  
and whether they are impacted  
by data assimilation

141 **2.2 ERA-Interim**

142 We use 6-hourly vertical velocities from the European Centre for Medium-Range  
143 Weather Forecasts (ECMWF) Interim reanalysis (ERAi) from 1995 to 2015 (Dee *et al.*, 2011).  
144 The nearest grid points are taken for Gadanki (13.68°N, 79.45°E) and Kototabang (0.35°S,  
145 100.54°E). Although 37 pressure levels up to 1 hPa resolution are available, we have restricted  
146 the dataset to 21 km, as that is the maximum radar range.

147 **2.3 ERA5**

148 When compared to ERAi, the fifth ECMWF reanalysis (ERA5) provides much higher  
149 spatial (30 km) and temporal resolution (hourly) from the surface up to 80 km (137 levels).  
150 ERA5 also features much improved representation especially over the tropical regions of the  
151 troposphere and better global balance of precipitation and evaporation. Many new data types not  
152 assimilated in ERAi are ingested in ERA5 (Hoffmann *et al.*, 2018). The details are available in  
153 Copernicus climate change service report (Hersbach and Dee 2016 and  
154 <https://cds.climate.copernicus.eu/cdsapp#!/home>). The nearest grid points are again taken for  
155 Gadanki (13.63°N, 79.31°E) and Kototabang (0.14°S, 100.40°E), and the data period is 2002-  
156 2015.

157 **2.4 MERRA-2**

158 The Modern Era Retrospective analysis for Research and Applications, version 2  
159 (MERRA-2) is the latest reanalysis of the modern satellite era produced by the National  
160 Aeronautics and Space Administration's (NASA) Global Modelling and Assimilation Office  
161 (GMAO). MERRA-2 data are provided on 42 pressure levels from the surface to 0.01 hPa with a  
162 temporal resolution of 3 h and horizontal resolution of 0.5° in latitude by 0.625° in longitude.  
163 Details have been provided by Gelaro *et al.* (2017). The nearest grid points are used for Gadanki  
164 (13.5°N, 79.37°E) and Kototabang (0.14°S, 100.00°E), with coverage from 1995 to 2015.



165 **2.5 NCEP-2** 15

166 The National Centers for Environmental Prediction – National Center for Atmospheric  
167 Research (NCEP-NCAR) reanalysis is based on the NCEP operational model with a horizontal  
168 resolution of 209 km and 28 vertical levels. Its temporal coverage is four times per day. NCEP-2  
169 products are improved relative to NCEP-1, having fixed errors and updated parameterizations of  
170 physical processes, as evaluated by *Kanamitsu et al.* (2002). The data for the present study  
171 covers 1995 to 2015 and is extracted at the nearest grid points to Gadanki (12.5°N, 77.5°E) and  
172 Kototabang (0, 100.00°E) 16

173 **2.6 JRA-55**

174 The Japanese 55-year reanalysis (JRA-55) is an updated version of the earlier JRA-25  
175 with new data assimilation and prediction systems (*Kobayashi et al.*, 2015). New radiation  
176 schemes, higher spatial resolution and 4D-var data assimilation with variational bias correction  
177 for satellite radiances have been used to generate the JRA-55 products. This reanalysis includes  
178 variation in greenhouse gas concentrations with time, as well as the new representations of land  
179 surface parameters, aerosols, ozone and SSTs. The horizontal resolution of the forecast model is 17  
180 ~60 km for JRA-55. The nearest grid points are taken for Gadanki (13.75°N, 78.75°E) and  
181 Kototabang (0, 100°E) and the data period is 1995-2015.

182

183 For all the reanalyses data,  $w$  (in  $\text{cm s}^{-1}$ ) is estimated using the formula:

184 
$$w = -\frac{1}{g} \omega \frac{RT}{p} \quad (2)$$

185 where  $\omega$  is the vertical velocity in pressure coordinates (in  $\text{Pa s}^{-1}$ ),  $T$  is the absolute temperature  
186 (K),  $p$  is the atmospheric pressure (hPa) and  $R$  ( $=287 \text{ J kg}^{-1} \text{ K}^{-1}$ ) is the gas constant. To compare

18





187 measured vertical wind with the reanalysis products, we take ~~the~~ reanalysis data corresponding to  
188 12 GMT for Gadanki and the daily mean for Kototabang.

(19)

### 189 3 Results and Discussion

190 Figure 1 shows the climatological monthly mean altitude profile of  $w$  obtained from the  
191 IMSTR (observations) and the ERAi, ERA5, MERRA-2, NCEP-2 and JRA-55 <sup>reanalysis</sup> reanalysis data  
192 sets over Gadanki. Although the magnitudes are of the same order between the observations and  
193 reanalyses, <sup>(space)</sup> significant differences are identified in the figures. It is to be noted that convective  
194 days are discarded <sup>w</sup> <sup>from</sup> <sup>data?</sup> in the radar analysis (observations) as mentioned in the previous section, and  
195 those days are also eliminated from all ~~the~~ reanalysis data sets. These differences may be  
196 attributed to the spatial averaging implicit in the reanalysis products, whereas the radar  
197 measurements are for a single point. Thus in the present study, we only discuss the tendency of  $w$   
198 as it is used to represent the <sup>qualitative?</sup> global variation of  $w$ , rather than its magnitude. The IMSTR  
199 observations show updrafts between 8 and 20 km, with the largest values in the tropical  
200 tropopause layer (TTL, 12-16 km), from December to April. These features are not reproduced  
201 by any of the reanalyses, which all show downdrafts from December to April between 1 km and  
202 the tropopause level (mean tropopause is ~ 16.5 km). Comparatively, downdrafts are observed in  
203 the IMSTR below 6 km in April, which may be attributed to pre-monsoon (March-May)  
204 precipitation and evaporation (Uma and Rao, 2009a). Vertical velocity in ERAi differs in both  
205 magnitude and direction from other reanalyses, especially in the lower troposphere from March  
206 to June. Meanwhile, the magnitude of vertical velocity in ERA-5 <sup>(21)</sup> is a little larger / than that in the  
207 other reanalyses / from May to June. Updrafts are observed in the TTL by the IMSTR during  
208 June, when all reanalyses show similar features but located <sup>only?</sup> below the TTL. During July and  
209 August both the radar observations and the reanalyses show updrafts in the vicinity of the TTL.



210 Updrafts are observed in the TTL from September to November but the peak in the updrafts is  
211 shifted lower than that observed by the IMSTR. Below 8 km, IMSTR shows downdrafts from  
212 April to October. ~~It is notable that~~ <sup>the</sup> the reanalyses only produce downdrafts below 2 km and are  
213 unable to reproduce ~~the~~ downdrafts above 2 km. Earlier studies using the IMSTR showed similar  
214 seasonal characteristics for  $w$  (Rao *et al.*, 2008).

215 *Uma and Rao* (2009b) have reported the diurnal variation of  $w$  in different seasons, <sup>although</sup> their <sup>(23)</sup> their  
216 observations <sup>had</sup> have only 1-2 diurnal cycles per month over Gadanki. They found significant <sup>diurnal?</sup>  
217 <sup>the</sup> variations as large as 6 cm/s over Gadanki using IMSTR. The present observations are limited to  
218 16:30 to 17:30 IST, with all reanalysis data over Gadanki taken at 12 GMT (17:30 IST). Thus,  
219 time-averaged climatological mean biases can be neglected. We have also analyzed  $w$  from the  
220 EAR (Kototabang) where the observations are available for the full diurnal cycle (measurements <sup>(24)</sup>  
221 of hourly averages for 24 hrs of observations). All reanalysis data over Kototabang are averaged  
222 for the full diurnal cycle. Figure 2 shows the monthly mean climatology of daily mean  $w$  ~~of~~  
223 <sup>from</sup> <sup>observations</sup> observed by the EAR and five reanalyses over Kototabang. All the reanalyses agree well with  
224 each other over Kototabang. Radar measurements of  $w$  at this location consistently show updrafts  
225 <sup>the</sup> in TTL region and downdrafts below 6 km (e.g. Rao *et al.*, 2008). The updrafts in the TTL are  
226 well reproduced by all <sup>five</sup> the reanalyses, although the ~~peak~~ <sup>of  $w$</sup>  magnitude ~~of  $w$~~  and ~~its~~ vertical location <sup>of</sup>  
227 <sup>the maximum in  $w$</sup>  remain lower than observed. However none of the reanalyses reproduces the downdrafts. A  
228 distinct bimodal distribution in  $w$  from May to September (two peaks between 8-10 km and 14-  
229 17 km) with a local minimum between 12 and 13 km is observed in the EAR measurements. The  
230 magnitudes of both updrafts and downdrafts are larger than those observed over Gadanki. JRA-  
231 55 produces the largest  $w$  among the reanalyses. The monthly means show significant differences  
232 in the direction of  $w$  between the observations and the reanalyses below 6 km. <sup>(25)</sup>



233 To establish the robustness of the results ~~obtained from both the observations and~~  
234 ~~reanalyses~~ we have used different averaging procedures to assess the consistency of the  
235 variability in  $w$  at monthly scales. Monthly mean climatological profiles of  $w$  from radar  
236 observations and various reanalyses over Gadanki and Kototabang ~~respectively~~ are shown in  
237 Figure 3. Downdrafts in the troposphere are not captured by any of the reanalyses over either  
238 location. By contrast, updrafts in the TTL are generally reproduced in the monthly mean, though  
239 ~~they~~ <sup>their magnitudes</sup> are often overestimated by the reanalyses. ERAi underestimates the magnitudes of both  
240 updrafts and downdrafts over Gadanki, ~~and~~ while NCEP-2 underestimates the magnitude of  
241 updrafts over Kototabang.

242 Monthly means calculated over five-year periods from both <sup>the data</sup> radar and ERAi are shown in  
243 Figure 4 for Gadanki and Figure 5 for Kototabang. The reanalysis shows a similar behavior to  
244 the overall climatology in each five-year average. The overall patterns of updrafts and  
245 downdrafts in the radar measurements of vertical velocity are also similar, indicating a consistent  
246 performance of the radar over the full 20 year analysis period.

247 To further elucidate potential biases in the results due to averaging, we have taken <sup>ERA5</sup> ERA-5  
248 at 12 GMT and compared it to the daily mean (obtained by averaging  $w$  at different times of the  
249 day) <sup>26</sup> to show that the sampling restrictions at Gadanki do not bias the results obtained. Figures 6  
250 and 7 show the mean  $w$  obtained at 12 GMT and also the mean obtained by averaging hourly  
251 analyses for each day for Gadanki and Kototabang, respectively. ERA5 is chosen for this  
252 evaluation as the data are available at one-hour interval. <sup>some differences</sup> The analysis shows <sup>in</sup> the magnitude of  
253  $w$ , with 12 GMT generally showing larger magnitudes compared to the daily means over  
254 Gadanki (although no such systematic differences is observed <sup>in</sup> in Kototabang). The directional



255 tendencies are also similar in both the profiles at both locations. This analysis shows that the  
256 results are not biased by taking data only at 12 UTC over Gadanki.

257 Our analysis to this point shows the level of consistency between the features observed  
258 by the radar and <sup>those in</sup> the reanalyses. To further understand the relative differences among the  
259 reanalyses we perform a monthly mean comparative analysis among the reanalyses, as shown in  
260 Figure 8. In this case, we <sup>take</sup> ERAi as a reference and compare it with  $w$  products from other  
261 reanalyses. We <sup>choose</sup> ERAi because the zonal and meridional winds from this reanalysis have  
262 been shown to compare well with radiosonde and rocket sounding observations over the Indian  
263 equatorial region (*Das et al.*, 2015). The solid lines in Figure 8 show ~~the~~ differences over  
264 Gadanki, while the dashed lines show differences over Kototabang. Over Gadanki, the difference  
265 between ~~the~~ ERAi and <sup>the</sup> other reanalyses is less than  $\pm 0.5$  cm/s during December-January-  
266 February (DJF, winter). ERAi underestimates ERA5 compared to other reanalyses, while values  
267 based on MERRA-2 are <sup>relative to</sup> ~~relatively larger than~~ those in other reanalyses. During MAM, strong  
268 downdrafts are found below 5 km with comparable magnitudes in all five reanalyses. ERAi  
269 underestimates ERA5 and NCEP-2 during March, and all other reanalyses from April to  
270 September. Values of  $w$  in ERAi are larger than those in NCEP-2 above 8 km. All five  
271 reanalyses compare well at all <sup>altitudes</sup> ~~altitudes~~ above 18 km. As expected, magnitudes are larger during  
272 JJA than during other months. From October to November, the magnitude ~~reduces to~~  $\pm 1$  cm/s

273 with values from ERAi smaller than those from all other reanalyses except NCEP-2.  
274 ~~Over Kototabang,~~ <sup>Over Kototabang</sup> the magnitude of  $w$  is ~~relatively~~ larger than over Gadanki. ~~It is~~  
275 ~~interesting to note that,~~ ERAi underestimates MERRA-2 in all months over this location <sup>as well</sup> ~~also~~  
276 (MERRA-2 shows larger magnitudes compared to other reanalyses). Similarly values based on  
277 ERAi are larger than those based on NCEP-2. From December to February ERAi underestimates

ERAi

27



28

278 MERRA-2 below 10 km and ERA5 between 10 and 15 km while overestimates NCEP-2 and  
279 JRA-55. The overall bias pattern remains the same during MAM, except for differences relative  
280 to JRA-55. From June–November, ERAi underestimates NCEP-2 and overestimates all the other  
281 three reanalyses.

282 The direction of  $w$  is an essential metric for comparing the observations <sup>reanalyses with?</sup> and ~~reanalyses~~.  
283 We therefore show the directional tendencies from the IMSTR and the EAR measurements ~~with~~  
284 relative to those from the reanalysis data. Figure 9a shows the directional tendencies based on the  
285 IMSTR and the reanalyses over Gadanki, while Figure 9b shows the directional tendencies based  
286 on the EAR and the reanalyses over Kototabang. The directional tendency is calculated at each  
287 height for every month when the radar or reanalysis data exceed 1 cm/s in either direction. The  
288 directional tendency for each month is estimated and then aggregated into seasons. These  
289 directional tendencies are given in terms of percentage of occurrence with respect to height. The  
290 directional tendency is calculated for  $w$  only if the magnitudes lie above  $\pm 0.1$  cm/s for both radar  
291 retrievals and reanalyses. The tendency is calculated separately for updrafts and downdrafts.

292 <sup>30</sup> Over Gadanki during DJF all reanalyses produce updrafts at rates of less than 10 % of  
293 <sup>29</sup> updrafts throughout the profile. During MAM these ratios increase to 15 %, with NCEP-2  
294 producing updrafts about 25 % of the time. During JJA and SON, the percentage occurrence  
295 increases with height from 25 % to a maximum of 50 % between 12 and 14 km. The percentage  
296 of updrafts occurrence then decreases from 14 to 20 km. This tendency trend is similar for all ~~the~~  
297 reanalyses except ERA5, for which the percentage occurrence is less than 25 % <sup>frequency?</sup> ~~during~~ all  
298 seasons. The maximum ratio of updrafts over Gadanki is located between 12 and 15 km altitude.

299 The percentage occurrence of downdrafts over Gadanki is also less than 50 % at all ~~the~~  
300 levels. During DJF and MAM the reanalyses produce downdrafts 40 to 50 % of the time, a much



301 higher frequency <sup>than that for</sup> compared to the updrafts (<10 %). <sup>(31)</sup> However, these ratios decrease above 10  
302 km. By contrast, the percentage of downdrafts produced during JJA and SON is less than that of  
303 ~~the~~ updrafts, with frequencies less than 25 % <sup>at</sup> in all ~~the~~ levels during these seasons. The  
304 performance of ERA5 over Gadanki <sup>appears to be</sup> is very poor as the occurrence frequencies are very small for both  
305 updrafts and downdrafts. [c]

306 Over Kototabang the percentage occurrence of updrafts increases with height in all  
307 seasons, reaching a maximum of 75- 90 % between 10 and 14 km. Above 14 km the percentage  
308 decreases to a minimum of 5 % at 19 km. Updrafts are rarely produced by the reanalyses <sup>at</sup>  
309 altitudes less than 4 km. It is important to note that none of the reanalyses produce daily mean  
310 downdrafts exceeding 1 cm/s between 6 and 16 km. The percentage of downdrafts increases both  
311 below 6 km and above 17 km, where it reaches <sup>(32)</sup> a maximum of about 25 to 50 %. MERRA-2,  
312 NCEP-2 and JRA-55 show occurrence frequencies of downdrafts around 65 to 75 % above 18  
313 km. The performance of ERA5 appears to be poor compared to the other reanalyses over this  
314 location as well. [c]

#### 315 4 Summary

316 The present study assesses the vertical motion ( $w$ ) in reanalyses against direct radar  
317 observations from the convectively active regions Gadanki and Kototabang. The assessment is  
318 carried out for five different reanalyses: ERA-Interim, ERA-5, MERRA-2, NCEP-2 and JRA-55.  
319 Measurements were collected using VHF radar at both locations. We have used 20 years of data  
320 from Gadanki and 17 years of data from Kototabang. The following points summarize the results  
321 of this unique study

322 a. The magnitude of  $w$  obtained from reanalyses is underestimated by 10-50% relative to the  
323 radar observations.



324 b. Observations over Gadanki showed updrafts from 8 to 20 km <sup>year-round</sup> year around. The reanalyses  
325 only reproduced this feature during JJA and SON when magnitudes were larger than 0.5 cm/s  
326 in the reanalyses. However, the vertical location of the updrafts differs between the  
327 observations and the reanalyses. Downdrafts below 8 km are not captured well by reanalyses.  
328 c. Over Kototabang, the reanalyses did not consistently <sup>reproduce?</sup> produce downdrafts below 8 km in all  
329 months. Updrafts in the UTLS are captured well; however, the peak in the vertical  
330 distribution of  $w$  is different as over Gadanki. (33)  
331 d. Inter-comparison among the reanalyses shows that ERAi overestimates NCEP-2 and  
332 underestimates the other three reanalyses with respect to the magnitude of  $w$  over both (34)  
333 Gadanki and Kototabang.  
334 e. Assessment of directional tendencies shows that updrafts are reproduced reasonably well in  
335 all ~~the~~ five reanalyses but downdrafts are not reproduced at all.  
336 Our analysis reveals that downdrafts are not well <sup>captured</sup> produced in reanalyses, ~~and also~~ the location of  
337 the largest updrafts is <sup>also</sup> shifted lower <sup>in reanalyses</sup> than in the observations. Hence, ~~the~~ reanalyses should be used  
338 with care for representing various atmospheric motion calculations (viz. diabatic heating,  
339 convection, etc.) that mainly depend on the direction of  $w$ . This study provides the reanalysis (35)  
340 community an initial basis to improve the methodology for calculating  $w$  in reanalyses, as this is  
341 a much sought-parameter for atmospheric circulation calculations and analyses. (D)

342

### 343 Acknowledgements

344 Authors would like to acknowledge all the technical and scientific staffs of National  
345 Atmospheric Research Laboratory (NARL) and Research Institute of Sustainable Humanosphere  
346 (RISH), who directly or indirectly involved in the radar observations. Thanks to all the reanalysis



347 data centre for providing the data through the portal of Research data archival (RDA) of  
348 NCEP/UCAR. One of the author KVS thank Indian Research Organisation for providing  
349 research associateship during this study.

350

351 **Data availability:** Analysed data (both radars and reanalyses) used in this study can be obtained  
352 on request. Raw time series data are available through open access in the following websites:

353 For Indian MST Radar : [www.narl.gov.in](http://www.narl.gov.in)

354 For EAR radar : [www.rish-kyoto-u.ac.jp/ear/index-e.html](http://www.rish-kyoto-u.ac.jp/ear/index-e.html)

355 For ERAi, ERA-5, JRA-55 and NCEP-2.: <https://rda.ucar.edu>

356 For MERRA-2 : <https://disc.gsfc.nasa.gov.in>



### 357 **Author's Contributions**

358 KNU conceived the idea for validation of vertical velocity among the reanalyses. SSD, MVR,  
359 and KVS collected and analysed the MST radar spectrum data. All the authors contribute for  
360 generation of figures, interpretation and manuscript preparation. The data used in the present  
361 study can be obtained on request.

### 362 **Conflict of Interest**

363 The authors declare that there is no conflict of interest.

364

365

366

367

368

369





370 **References**

- 371 Anandan, V.K., Reddy, G.R., Rao, P.B.: Spectral analysis of atmospheric signal using higher  
372 orders spectral estimation technique, *IEEE Trans. Geosci. Remote Sens.*, 39, 1890.  
373 doi:10.1109/36.951079, 2001.
- 374 Back, L. E., and C.S. Bretherton.: Geographic variability in the export of moiststatic energy  
375 and vertical motion profiles in the tropical Pacific, *Geophys. Res. Lett.*, 33, L17810,  
376 doi:10.1029/2006GL026672, 2006.
- 377 Das, S. S., K. N. Uma, V. N. Bineesha, K. V. Suneeth and G. Ramkumar.: Four decadal  
378 climatological intercomparison of rocketsonde and radiosonde with different reanalysis  
379 data: results from Thumba Equatorial Station, *Q. J. Roy. Met. Soc.*, DOI:10.1002/qj.2632,  
380 2015.
- 381 Dee D. P et al.: The ERA-Interim reanalysis: Configuration and performance of the data  
382 assimilation system. *Q. J. R. Meteorol. Soc.*, 137, 553–597, doi: 10.1002/qj.828, 2011.
- 383 Dowdy, A., R. A. Vincent, K. Igarashi, Y. Murayama and D.J. Murphy.: A comparison of mean  
384 winds and gravity wave activity in the northern and southern polar MLT. *Geophys. Res. Lett.*,  
385 28( 8), 1475- 1478. <https://doi.org/10.1029/2000GL012576>, 2001
- 386 Fukao, S., H. Hashiguchi, M. Yamamoto, T. Tsuda, T. Nakamura, M. K. Yamamoto, T. Sato, M.  
387 Hagio, and Y. Yabugaki.: Equatorial Atmosphere Radar (EAR): System description and first  
388 results, *Radio Sci.*, 38(3), 1053, doi:10.1029/2002RS002767, 2003.
- 389 Fujiwara, M., Wright, J. S., Manney, G. L., Gray, L. J., Anstey, J., Birner, T., Davis, S., Gerber,  
390 E. P., Harvey, V. L., Hegglin, M. I., Homeyer, C. R., Knox, J. A., Krüger, K., Lambert, A.,  
391 Long, C. S., Martineau, P., Molod, A., Monge-Sanz, B. M., Santee, M. L., Tegtmeier, S.,  
392 Chabrillat, S., Tan, D. G. H., Jackson, D. R., Polavarapu, S., Compo, G. P., Dragani, R.,



- 393 Ebisuzaki, W., Harada, Y., Kobayashi, C., McCarty, W., Onogi, K., Pawson, S., Simmons,  
394 A., Wargan, K., Whitaker, J. S., and Zou, C.-Z.: Introduction to the SPARC Reanalysis  
395 Intercomparison Project (S-RIP) and overview of the reanalysis systems, *Atmos. Chem.*  
396 *Phys.*, 17, 1417–1452, <https://doi.org/10.5194/acp-17-1417-2017>, 2017.
- 397 Gelaro, et al.: The Modern-Era Retrospective Analysis for Research and Applications, Version 2  
398 (MERRA-2), *J. Clim.*, 30, 5419–5454, doi: 10.1175/JCLI-D-16-0758.1, 2017.
- 399 Hersbach, H. and Dee, D.: ERA5 reanalysis is in production, *ECMWF Newsletter*, Vol. 147, p.  
400 7, available at: <https://www.ecmwf.int/en/newsletter/147/news/era5-reanalysis-production>,  
401 2016.
- 402 Hoffmann, L., Günther, G., Li, D., Stein, O., Wu, X., Griessbach, S., Heng, Y., Konopka, P.,  
403 Müller, R., Vogel, B., and Wright, J. S.: From ERA-Interim to ERA5: the considerable  
404 impact of ECMWF's next-generation reanalysis on Lagrangian transport simulations, *Atmos.*  
405 *Chem. Phys.*, 19, 3097–3124, <https://doi.org/10.5194/acp-19-3097-2019>, 2019.
- 406 Huaman, M., and B. B. Balsley.: Long-term average vertical motions observed by VHF wind  
407 profilers: The effect of slight antenna pointing inaccuracies, *J. Atmos. Oceanic Technol.*, 13,  
408 560–569, 1996.
- 409 Kanamitsu M, W. Ebisuzaki, J. Woollen, S. K. Yang, J. J. Hnilo, M. Fiorino, G. L. Potter.:  
410 NCEP-DOE AMIP-II reanalysis (R-2). *Bull. Am. Meteorol. Soc.*, 83: 1631–1643, doi:  
411 10.1175/BAMS-83-11-1631, 2002.
- 412 Kennedy, A. D., X. dong and B. Xi.: Comparison of MERRA and NARR Reanalyses with the  
413 DOE ARM SGP Data, *J. Clim.*, DOI: 10.1175/2011JCLI3978.1, 2012.
- 414 Kobayashi, S., et al.: The JRA-55 Reanalysis: General specifications and basic characteristics, *J.*  
415 *Meteorol. Soc. Jp.*, 93, doi:10.2151/jmsj.2015-001, 2015.



- 416 Laskar, F. I., et al.: Experimental evidence of arctic summer mesospheric upwelling and its  
417 connection to cold summer mesopause, *Geophys. Res. Lett.*, 44, 9151- 9158.  
418 doi:10.1002/2017GL074759, 2017
- 419 Liou, Y.C., and Chang., Y. J.: A Variational Multiple-Doppler Radar Three-Dimensional Wind  
420 Synthesis Method and Its Impacts on Thermodynamic Retrieval, *Mon. Wea. Rev.*, 137:11,  
421 3992- 4010, 2009.
- 422 Matejka, T.: Estimating the most steady frame of reference from Doppler radar data, *J. Atmos.*  
423 *Oceanic Technol.*, 19, 1035-1048, 2002.
- 424 Nastrom, G. D., and T. E. VanZandt.: Mean vertical motions seen by radar wind profilers, *J.*  
425 *Appl. Meteorol.*, 33, 984–995, 1994.
- 426 Peterson, V. L., and B. B. Balsley.: Clear air Doppler measurements of the vertical component of  
427 wind velocity in the troposphere and stratosphere. *Geophys. Res. Lett.*, 6(12), 1979,
- 428 Rao, P. B., A. R. Jain, P. Kishore, P. Balamuralidhar, S. H. Damle, and G. Viswanathan.: Indian  
429 MST radar 1. System description and sample vector wind measurements using ST mode,  
430 *Radio Sci.*, 30, 1125–1138, 1995.
- 431 Rao, T.N, K. N. Uma, D. Narayana Rao, and S. Fukao.: Understanding the transportation process  
432 of tropospheric air entering the stratosphere from direct vertical air motion measurements  
433 over Gadanki and Kototabang, *Geophys. Res. Lett.*, 35, L15805,  
434 doi:10.1029/2008GL034220, 2008.
- 435 Rao, T. N., Uma, K. N, T. M. Satyanarayana and D. N. Rao.: Differences in Draft Core Statistics  
436 from the Wet to Dry Spell over Gadanki, India (13.5°N, 79.2°E), *Mon.Wea.Rev.*, 137, 4293-  
437 4306, DOI: 10.1175/2009MWR3057.1, 2009.



- 438 Rao, T. N., K. K. Kumar, S. S., Das, T. N. Rao, T. M. Satyanarayana.: On the Vertical  
439 Distribution of Mean Vertical Velocities in the Convective Regions during the Wet and  
440 Dry Spells of the Monsoon over Gadanki, *Mon.Wea.Rev.*, 140, 398-410, 2011.
- 441 Rao, V., D. Rao, M. V. Ratnam, K. Mohan, and S. Rao.: Mean Vertical Velocities Measured by  
442 Indian MST Radar and Comparison with Indirectly Computed Values, *J. App. Meteo*, 42(4),  
443 541-552. Retrieved from <http://www.jstor.org/stable/26185424>, 2003.
- 444 Stepanyuk, O., R. Jouni, V. Sinclair, Heikki, , Järvinen.: Factors affecting atmospheric vertical  
445 motions as analyzed with a generalized omega equation and the OpenIFS model. *Tellus.*, 69,  
446 1271563. 10.1080/16000870.2016.1271563, 2017.
- 447 Tanaka, H. L., and A. Yatagai.: Comparative study of vertical motions in the global atmosphere  
448 evaluated by various kinematic schemes, *J. Meteo.Soc.Jp.*, 78, 289-298, 2000.
- 449 Uma, K. N., and Rao, T. N.: Characteristics of Vertical Velocity Cores in Different Convective  
450 Systems Observed over Gadanki, India, *Mon.Wea.Rev.*, 137, 954-974, DOI:  
451 10.1175/2008MWR2677.1, 2009a.
- 452 Uma, K. N., and Rao, T. N.: Diurnal variation in vertical air motion over a tropical station,  
453 Gadanki (13.5°N, 79.2°E), and its effect on the estimation of mean vertical air motion, *J.*  
454 *Geophys. Res.*, 114, D20106, doi:10.1029/2009JD012560, 2009b.
- 455 Uma, K. N., Kumar, K. K., Das, S.S., Rao, T. N., and Satyanarayana, T. M.: On the Vertical  
456 Distribution of Mean Vertical Velocities in the Convective Regions during the Wet and Dry  
457 Spells of the Monsoon over Gadanki, *Mon. Weather Rev.*, 140, 398-410,  
458 <https://doi.org/10.1175/MWR-D-11-00044.1>, 2011.



459 Yamamoto, M. K., N. Nishi, T Horinouchi, M Niwano, and S Fukao.: Vertical wind observation  
460 in the tropical upper troposphere by VHF wind profiler: A case study, Rad, Sci., 42, RS3005,  
461 doi: 10.1029/2006RS003538, 2007.

462

463

464

465

466

467

468

469

470

471

472

473

474

475

476

477

478

479

480

481

482

483



484 **Figure Captions**

485 **Figure 1.** Climatological monthly mean altitude profile of vertical velocity obtained from MST  
486 Radar and 5-reanalysis at 12 GMT over Gadanki. Horizontal lines indicate the standard error.

487 **Figure 2.** Same as Fig.1, but for diurnal mean over Kototabang.

488 **Figure 3 :** Monthly mean climatology of vertical velocity obtained from (a) radars, (b) ERAi, (c)  
489 ERA-5, (d) MERRA-2, (e) NCEP-2, and JRA-55 over Gadanki (left) and Kototabang (right).  
490 Gadanki data are at 12 GMT and Kototabang data are diurnal mean.

491 **Figure 4.** Monthly mean vertical velocity obtained from (a) MST Radar and (b) ERAi for 5  
492 years interval (from top to bottom) over Gadanki (12 GMT).

493 **Figure 5.** Same as Fig.4 but for diurnal mean over Kototabang.

494 **Figure 6.** Height profile of vertical velocity at 12 GMT and diurnal mean (with 1 hour  
495 resolution) over Gadanki extracted from ERA-5 (highest available time resolution).

496 **Figure 7.** Same as Figure 6 but over Kototabang.

497 **Figure 8.** Comparison of relative differences in vertical velocity ( $w$ ) between the reanalysis for  
498 Gadanki (solid line) and Kototabang (dash line). Individual month differences are estimated and  
499 then averaged for each month. Over Gadanki, data is taken for 12 GMT and for Kototabang it is  
500 diurnal.

501 **Figure 9.** Comparison of directional tendency simultaneously observed in radar and various  
502 reanalysis data sets for (a) Gadanki and (b) Kototabang. Updrafts are shown in top and third  
503 panels and downdrafts are shown in middle and bottom panels (for details see text).



**Figure 1.** Climatological monthly mean altitude profile of vertical velocity obtained from <sup>the</sup> MST Radar and five reanalyses over Gadanki at 12 UTC. Horizontal lines indicate the standard error in each data set.

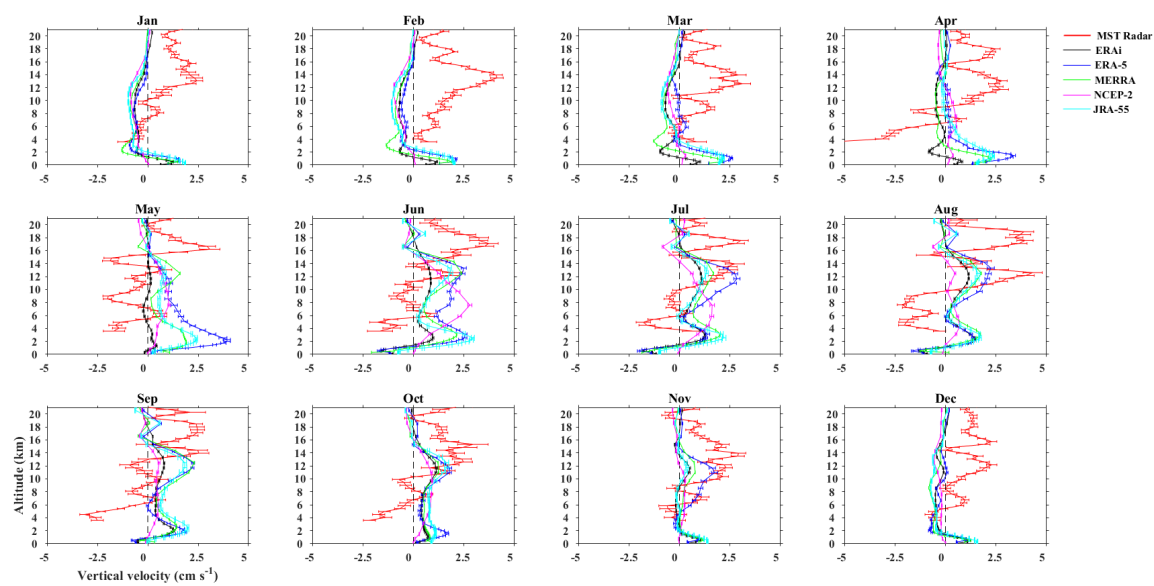




**Figure 2.** Same as Fig. 1, but for daily mean profiles over Kototabang.

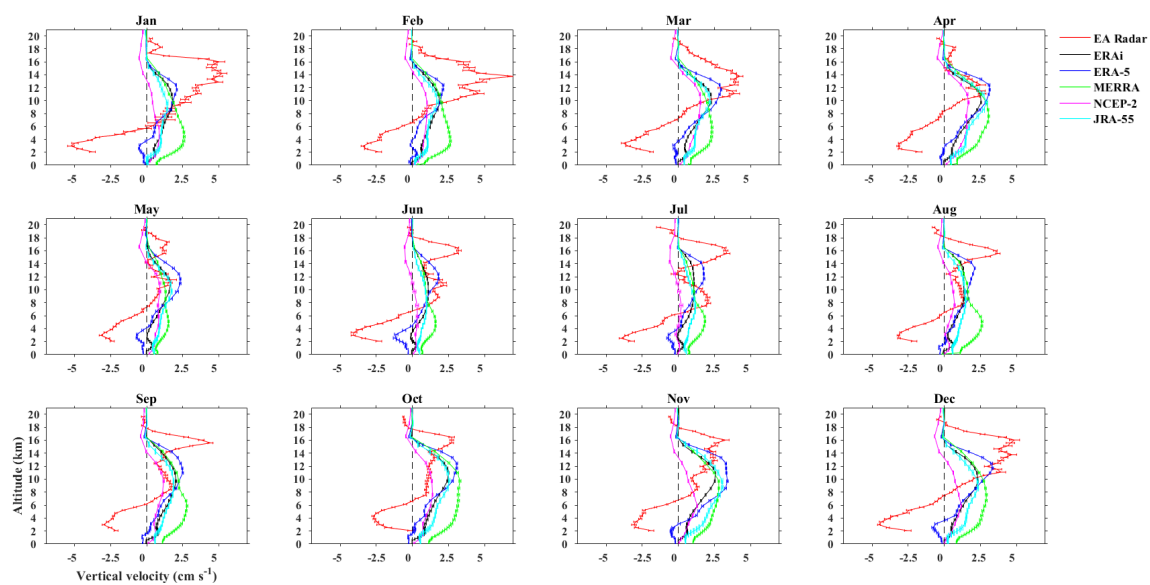






**Figure 3 :** Monthly mean climatologies of vertical velocity obtained from (a) radars, (b) ERAi, (c) ERA5, (d) MERRA-2, (e) NCEP-2, and JRA-55 over Gadanki (left) and Kototabang (right). Gadanki data are at 12 GMT and Kototabang data are daily means.

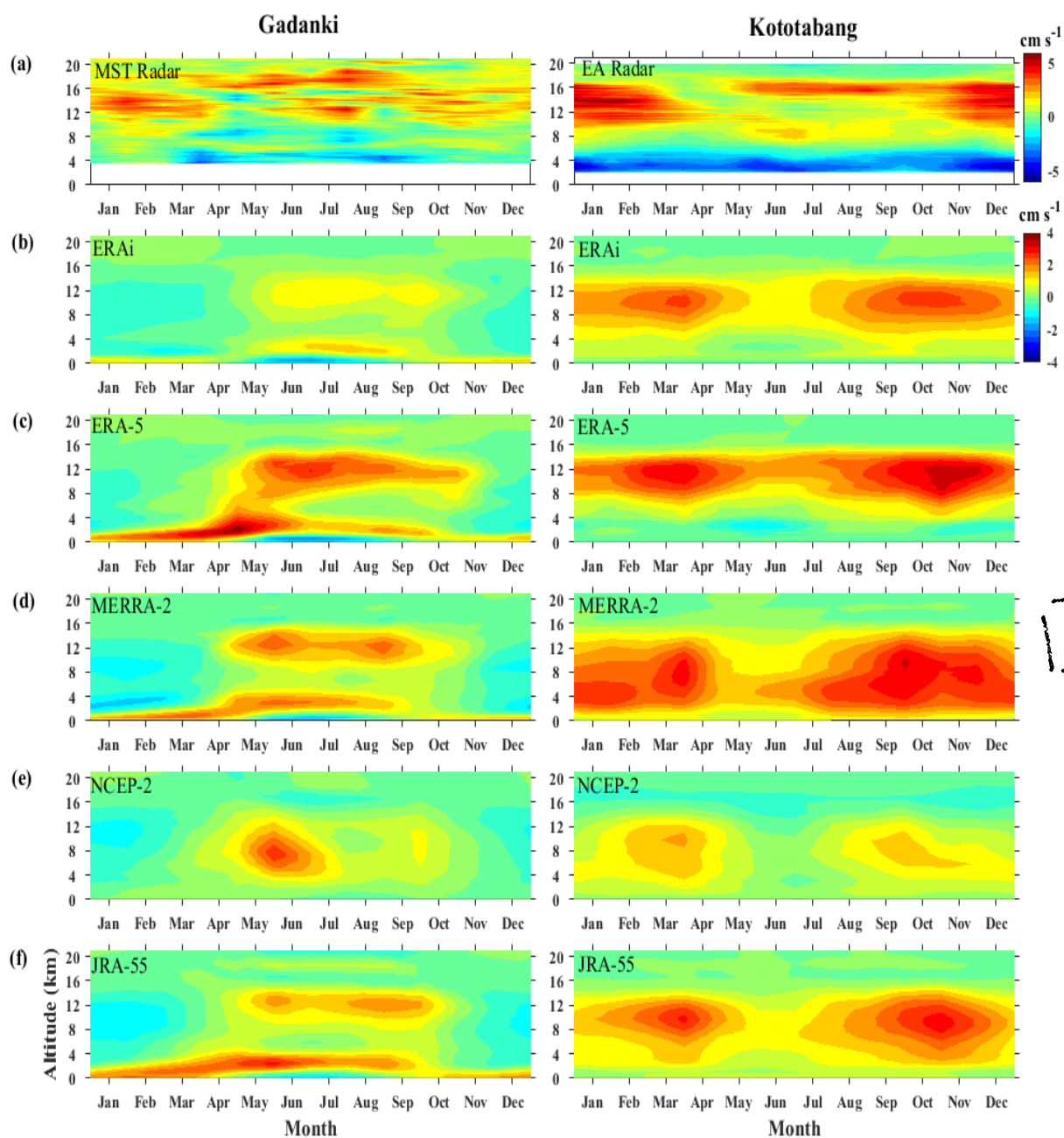




**Figure 4.** Monthly mean vertical <sup>velocities</sup> velocity obtained from (a) MST Radar and (b) ERAi for 5- <sup>in</sup> years intervals (from top to bottom) over Gadanki (12 GMT).

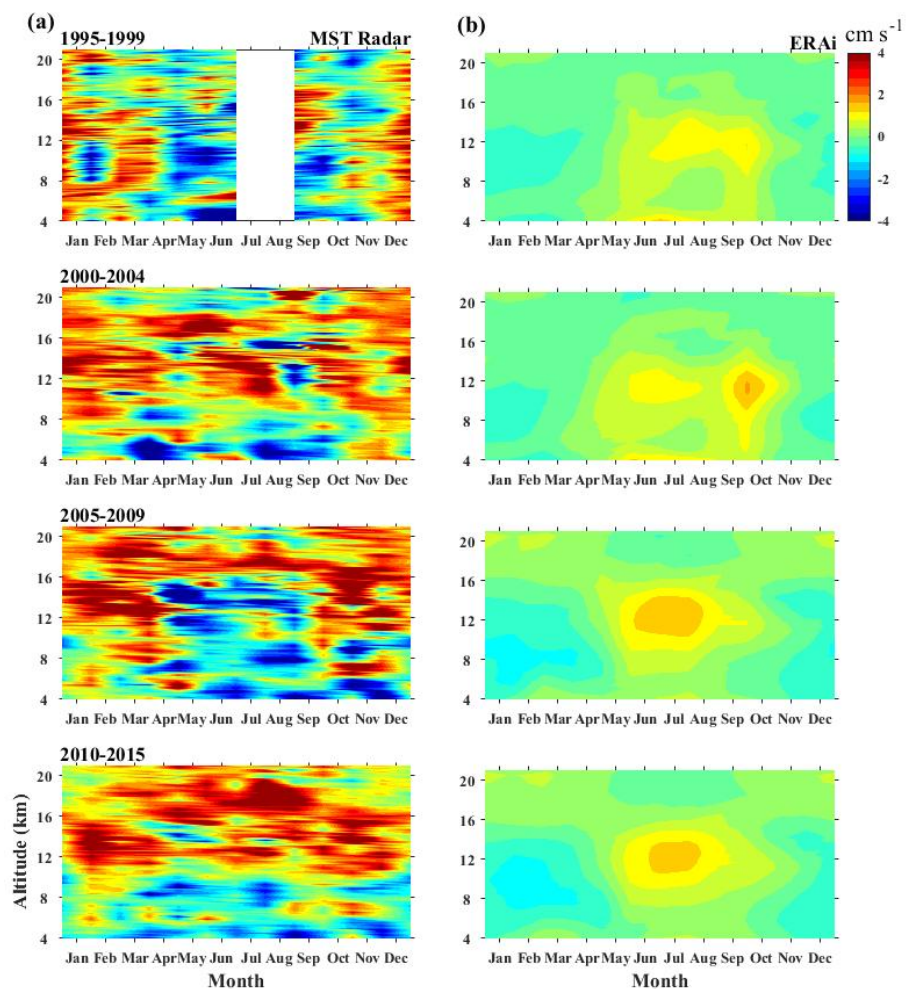
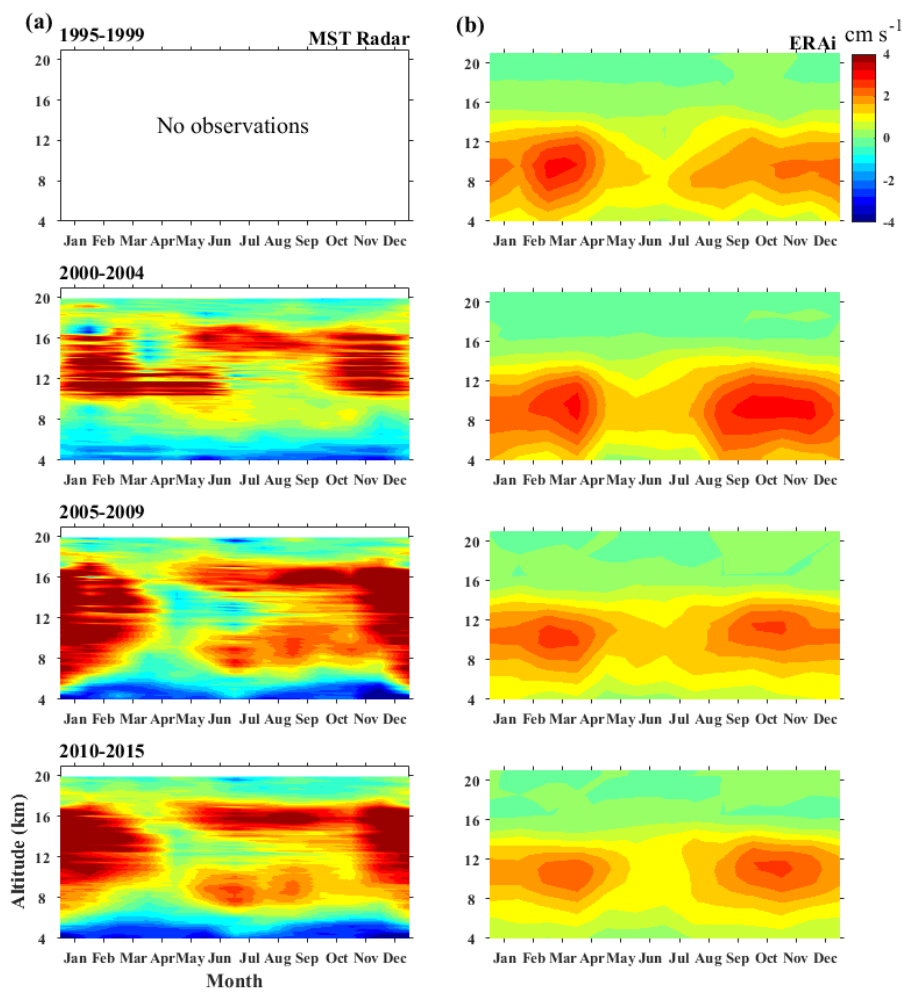


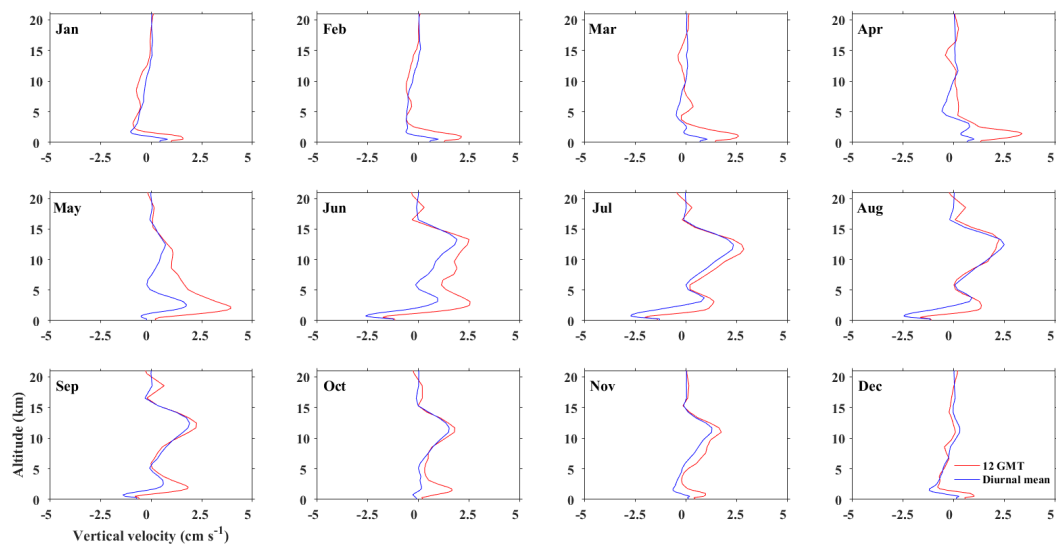


Figure 5. Same as Fig.S2 but for daily means over Kototabang.



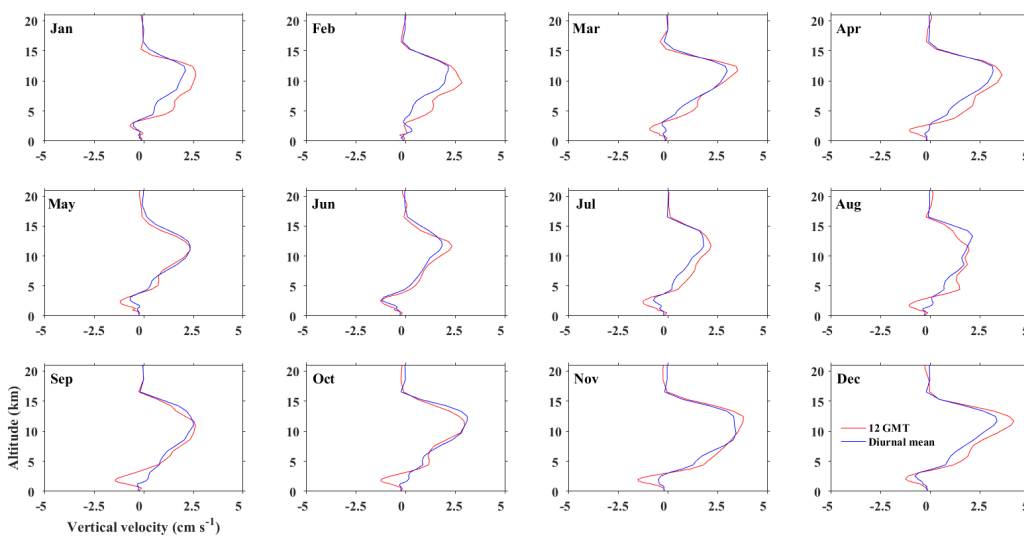


**Figure 6.** Height profiles of vertical velocity for 12 GMT and from daily mean (with 1 hour resolution) over Gadanki extracted from ERA5 (highest available time resolution).





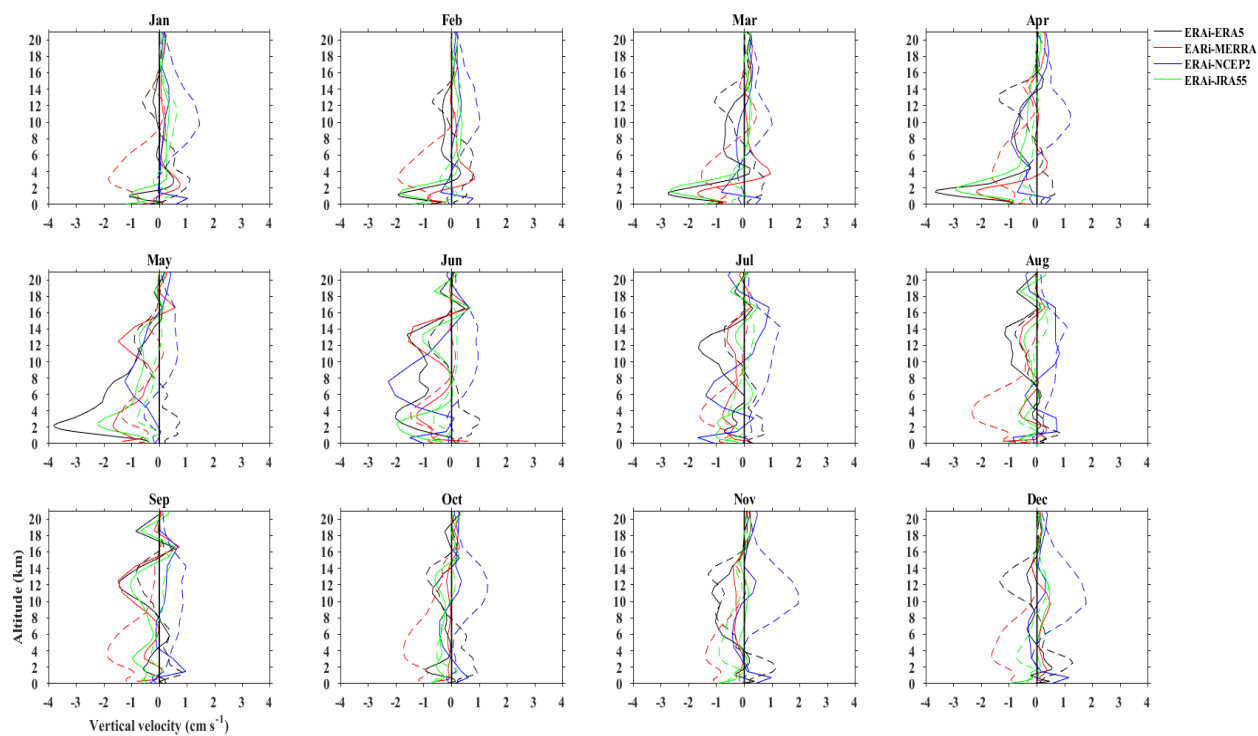
**Figure 7.** Same as Fig.6, but for Kototabang.





9

**Figure 8.** Comparison of relative differences in vertical velocity ( $w$ ) between the reanalysis for Gadanki (solid line) and Kototabang (dash line). Individual month differences are estimated relative to ERAi and then averaged for each month.





H

**Figure 9.** Comparison of directional tendencies between the radars and various reanalysis data sets for (a) Gadanki and (b) Kototabang. Updrafts are shown in the upper panels and downdrafts are shown in the lower panels for each site (for details see text).

